Available online at www.sciencedirect.com
SCIENCE DIRECT
Catalysis Today 114 (2006) 40–47
CATALYSIS TODAY
www.elsevier.com/locate/cattod

Promotional effect of rare earths and transition metals in the combustion of diesel soot over CeO_2 and CeO_2–ZrO_2

Eleonora Aneggi *, Carla de Leitenburg, Giuliano Dolcetti, Alessandro Trovarelli [1]

Dipartimento di Scienze e Tecnologie Chimiche, via Cotonificio 108, Università di Udine, 33100 Udine, Italy

Available online 20 March 2006

Abstract

The soot combustion behavior and the textural and structural characteristics of CeO_2 and a series of ceria-modified materials have been studied. It is shown that ceria doped with transition metals (Zr and Fe) and rare earth elements (La, Pr, Sm, Tb) results in more active catalysts with enhanced textural properties. ZrO_2 enhances the thermal stability and the oxygen storage capacity of pure ceria, resulting in better performance in soot oxidation. Remarkably, cerium–zirconium solid solution doped with rare earth does not achieve lower temperature of combustion, providing performances comparable to CeO_2 and CeO_2–ZrO_2. Cerium doped with Fe_2O_3 presents the better results as far as fresh samples are taken into account, but suffers from a net loss of activity after calcination. TGA experiments under N_2 atmosphere have confirmed the key role of oxygen storage capacity in soot oxidation.

Keywords: Ceria; Ceria–zirconia; Fe_2O_3; Soot oxidation; Diesel; Oxygen storage; Combustion

1. Introduction

Among the several techniques that have been developed for reducing particulate emissions from diesel engines, filtering followed by catalytic oxidation is one of the more promising. The basic idea of catalytic approach consists in the use of a catalyst to achieve the onset of regeneration at a temperature comparable to that of exhaust gases. Unfortunately, this method is affected by several drawbacks [1]: (i) catalytic filter regeneration is made difficult by the very variable conditions of reaction; (ii) the process is quite slow because of the poor soot–catalyst contact; actually, the solid particles are immobile when deposited and due to their large size can not penetrate into catalyst's micropores or mesopores; (iii) the temperature in the exhaust gases may vary in a wide range (indicatively from 473 to 873 K), depending upon engine load. Consequently, a useful catalyst has to operate efficiently at low temperatures and also to be thermally stable.

Several catalyst formulations for soot oxidation have been studied in the last years, and the most promising are those based on Cu/K/M/(Cl) (where M is either V, Mo or Nb) [2–4], that have been investigated in detail due to their high activity at low temperature.

Regarding the intimate mechanism involved in the oxidation of carbon, several authors pointed out the importance of redox properties of the catalyst. That is, the effectiveness of the catalyst can be related to its ability to deliver oxygen from the lattice to the gas phase (or better to the solid carbon reactant) in a wide temperature range [1]. Recently, it has been reported that the use of supports based on cerium oxide confers interesting properties to soot combustion catalysts due to high availability of surface oxygen and high surface reducibility [5–9]. The success of oxygen storage systems based on ceria is due to their ability to change oxidation state during operation (i.e. CeO_2 to CeO_{2-x}) maintaining structural integrity, thus allowing oxygen uptake and release to occur easily. State of the art material for oxygen storage in TWC is constituted by ceria and ceria–zirconia mixed oxides doped with small amounts of rare earth elements, added to enhance the redox features of ceria [10]. Homogeneity of solid solutions, structural features and composition are key parameters in successful redox catalyst design. Since it is being reported in the literature that a strong relationship exist between oxygen storage/redox capacity and

* Corresponding author. Tel.: +39 043 255 8865; fax: +39 043 255 8803.
E-mail address: Aneggi.Eleonora@spes.uniud.it (E. Aneggi).
[1] A member of CONCORDE, the EU-funded Coordination Action "Co-Ordination of Nanostructured Catalytic Oxides Research & Development in Europe".

0920-5861/$ – see front matter © 2006 Elsevier B.V. All rights reserved.
doi:10.1016/j.cattod.2006.02.008

soot combustion activity [11], it is of interest to investigate here if the knowledge that has been accumulated on redox systems for TWC can help in developing more active soot combustion catalysts.

In this study a series of ceria-based catalysts modified with rare earth (Sm, Pr, Tb, La) and transition metal elements (Zr, Fe) have been prepared and characterized from a structural and textural point of view. The effect of doping in the activity of soot combustion is also described by putting particular attention in correlating soot oxidation activity with oxygen storage and structural properties of the materials.

2. Experimental procedures

2.1. Catalyst preparation and characterization

Three classes of materials were prepared and characterized: ceria–zirconia solid solutions, ceria–zirconia doped with rare earth elements (La, Pr, Sm, Tb) and ceria and ceria–zirconia doped with Fe. They were prepared by coprecipitation starting from nitrates. Precipitates were dried at 393 K and calcined at 773 K for 2 h (fresh samples). Aged samples were prepared following calcination in air at 1023 K for 12 h. Chemical composition of all samples investigated is reported in Table 1.

Textural characteristics of all fresh and aged samples were measured according to the B.E.T. method by nitrogen adsorption at 77 K, using a Sorptomatic 1900 instrument (Carlo Erba).

Structural features of the catalysts were characterized by X-ray diffraction (XRD). XRD patterns were recorded on a Philips X'Pert diffractometer operated at 40 kV and 40 mA using nickel-filtered Cu Kα radiation. Spectra were collected using a step size of 0.02° and a counting time of 40 s per angular abscissa in the range 20–145°. The Philips X'Pert HighScore software was used for phase identification. The mean crystalline size was estimated from the full width at the half maximum (FWHM) of the X-ray diffraction peak using the Scherrer equation [12] with a correction for instrument line broadening. Rietveld refinement [13] of XRD pattern was performed by means of GSAS-EXPGUI program [14,15]. The accuracy of these values was estimated by checking their agreement against the values of the lattice constant, assumed to comply with the Vegard's law [16].

2.2. Catalytic activity

The catalytic activity for the combustion of soot was quantified by the peak-top temperature (T_m) during temperature programmed oxidation (TPO) of catalyst–soot mixtures [1,17–20]. Each catalyst was accurately mixed with soot in a mortar for 10 min in order to achieve a tight contact [21]. The kind of contact between catalyst and soot is extremely important [1,22]: the tight contact conditions are poorly representative of the real working conditions experienced by the catalyst deposited in a catalytic trap, but they allow a rapid screen of catalysts in reproducible experimental conditions.

A soot/catalyst weight ratio of 1:20 was adopted. During the TPO measurements 25 mg of mixture were heated at a constant rate (10 K/min) in a quartz reactor, while the gas flow (N_2 with 6% of O_2) was kept fixed at 400 ml/min. The catalyst temperature was checked by a chromel-alumel thermocouple, located on the catalyst bed. The outlet composition was measured by IR and paramagnetic gas analyzers (Magnos 106 and Uras14, ABB), by recording the percentages of CO, CO_2 and O_2 at the output of the reactor.

A series of tests were carried out for catalyst/soot mixtures, in order to verify the reproducibility of results; the peak temperatures show differences always lower than 5 K.

Soot oxidation activity was also tested by running TGA experiments (Q500, TA Instruments) either in the presence or in the absence of oxygen (N_2 atmosphere). In order to achieve the stoichiometric ratio between the amount of soot and the oxygen that the catalyst can donate, we used a soot/catalyst weight ratio of 1:115. The total flow of N_2 in the furnace was 100 ml/min. Samples were pre-treated for 1 h at 423 K to eliminate water absorbed, then they were heated at a constant rate (10 K/min) up to 1073 K; the weight loss of the sample, after subtraction of the blank, can be considered as an indication of activity of soot oxidation by oxygen from the catalyst.

Table 1
Characteristics of samples used in this study

Sample	Composition	B.E.T. surface area (m^2/g)		Crystallite size (nm)[a]		T_m (K)	
		Fresh	Aged	Fresh	Aged	Fresh	Aged
CZ100	CeO_2	57	22	7	11.2	662	700
CZ75	$Ce_{0.75}Zr_{0.25}O_2$	73	44	6.3	10	660	673
CZ44	$Ce_{0.44}Zr_{0.56}O_2$	96	54	4.7	13	675	674
CZ28	$Ce_{0.28}Zr_{0.72}O_2$	100	58	6.2	13	695	711
CZ0	ZrO_2	79	44	11.8	15.9	798	810
CF95	$Ce_{0.95}Fe_{0.05}O_{1.975}$	92	10	5.4	44.4	639	749
CF85	$Ce_{0.85}Fe_{0.15}O_{1.925}$	77	22	7.5	31.1	662	722
CZF95	$Ce_{0.47}Zr_{0.48}Fe_{0.05}O_{1.975}$	106	25	3.9	8.8	672	715
CZF85	$Ce_{0.45}Zr_{0.40}Fe_{0.15}O_{1.925}$	132	22	3.5	8.9	684	716
CZLa	$Ce_{0.48}Zr_{0.50}La_{0.02}O_{1.99}$	93	54	4.0	5.6	687	685
CZPr	$Ce_{0.48}Zr_{0.50}Pr_{0.02}O_{1.99}$	99	55	4.1	6.1	683	678
CZSm	$Ce_{0.48}Zr_{0.50}Sm_{0.02}O_{1.99}$	92	50	4.3	6.4	684	679
CZTb	$Ce_{0.48}Zr_{0.50}Tb_{0.02}O_{1.99}$	96	50	4.2	6.3	687	691

[a] Calculated with Scherrer formula from X-ray diffraction patterns.

In order to evaluate the OSC of samples we carried out TGA experiments in Ar/H_2 (5%) flow (total flow 100 ml/min). Each sample was treated in N_2 atmosphere for 1 h at 553 K. Then, it was heated at a constant rate (10 K/min) till 673 K and kept at this temperature for 15 min, to eliminate the absorbed water. Finally Ar/H_2 mixture was introduced while keeping the temperature at 673 K for 30 min. The observed weight loss is due to oxygen removal by H_2 to form water, and it can be associated to total oxygen storage capacity at that temperature [23].

3. Results and discussion

3.1. Textural and structural characterization

Textural and structural characterization of all samples is reported in Tables 1 and 2. Fresh materials have surface area in the range 60–130 m^2/g. The effect of aging strongly affects pure ceria and Fe-modified catalysts, while sintering in ceria–zirconia is less important in accordance with its better thermal resistance [24]. The presence of rare earth elements within ceria–zirconia lattice does not modify stability of ceria–zirconia against surface area loss.

The structural features of all samples were analyzed by XRD. As shown in Table 2, XRD measurements suggest that for binary ceria–zirconia samples with cerium content greater than 50 mol% the formation of a cubic fluorite lattice is favored. This is in accordance with literature, where generally the limit for formation of a cubic (either cubic or tetragonal t'') solid solution is found at ca. 50 mol% CeO_2 [25]. Thus, all our cerias crystallize in a cubic fluorite structure of *Fm3m* symmetry with almost identical cell parameters. A similar situation is found with fresh and aged CZ75; both crystallize in a cubic structure with a smaller cell parameter than ceria, in agreement with the introduction of the smaller Zr^{4+} in the lattice. The value of $a = 5.370$ fits well with data reported previously [25–27]. No indication of phase splitting is detected after aging, which is in line with what found on ceria-rich samples after similar treatments [28]. This however cannot exclude that thermal treatment might induce some phase assessment at a nano-scale level, with small compositional variations, which have been indicated as responsible for enhancement of oxygen exchange in samples obtained using similar procedures [29]. In the range of composition 25–45 mol% CeO_2 good agreement between the refinement and a tetragonal structural model confirms that all samples belong to the t' tetragonal phase with space group $P4_2/nmc$. No peak splitting that would indicate the presence of two phases could be detected, and therefore, the diffraction patterns demonstrate the formation of a single solid solution-like ceria–zirconia phase. Again, this cannot exclude the presence of different arrangements of oxygen sublattice or the presence of a multi-phase system at a nanoscale level, not detected by XRD. After calcinations, only a slight modification of the structural parameter is observed which does not affect

Table 2
Crystallographic parameters of modified ceria samples as obtained from Rietveld refinement and Vegard law

Sample	Phase	Cell parameters			From Vegard law
		$a = b = c$ (Å)	$a' = b'$ (Å)	c (Å)	
Fresh samples					
CZ100	Cubic	5.411			5.411
CZ75	Cubic	5.370			5.341
CZ44	Tetragonal t'		5.251	5.346	5.253
CZ28	Tetragonal t'		5.177	5.261	5.207
CZ0	Monoclinic tetragonal	Not refined			5.127
CF95	Cubic	5.404			5.356
CF85	Cubic	5.396			5.243
CZF95	Cubic	5.273			5.225
CZF85	Cubic	5.295			5.143
CZLa	Cubic	5.300			5.285
CZPr	Cubic	5.297			5.282
CZSm	Cubic	5.290			5.277
CZTb	Cubic	5.286			5.273
Aged samples					
CZ100	Cubic	5.410			5.411
CZ75	Cubic	5.370			5.341
CZ44	Tetragonal t'		5.250	5.341	5.253
CZ28	Tetragonal t'		5.175	5.266	5.207
CZ0	Monoclinic tetragonal	Not refined			5.127
CF95	Cubic	5.409			5.356
CF85	Cubic	5.408			5.243
CZF95	Cubic	5.275			5.225
CZF85	Cubic	5.292			5.143
CZLa	Cubic	5.297			5.285
CZPr	Cubic	5.297			5.282
CZSm	Cubic	5.289			5.277
CZTb	Cubic	5.285			5.273

overall phase distribution. In summary, XRD characterization of binary ceria–zirconia solid solutions confirms the homogeneity of samples (within the limits outlined above) with the identification of mainly cubic and tetragonal t' phases, as generally reported for similar composition [30].

In fresh samples based on CeO_2 doped with Fe, XRD features allow to detect only the CeO_2 cubic phase *Fm*3*m* while Fe_2O_3 or other iron oxide phases are not visible. XRD peaks are broad and the values of crystallite size obtained according to Scherrer equation are about 54 Å for sample CF95 and 75 Å for sample CF85. After aging at 1023 K, peaks become more intense, clear and well defined for all Fe-containing samples. Aging is accompanied by a large drop in surface area and by a consequent increase of crystallite size (444 and 311 Å, respectively, for CF95 and CF85). After calcination, the XRD profile of CF samples shows peaks assigned to rhombohedral Fe_2O_3 (hematite) with *R*-3*c* symmetry. The lack of peak due to iron oxide in fresh CF samples could indicate the formation of solid solution between Ce and Fe. However, a comparison between the values of cell parameter with those expected if all the iron contained were dissolved in the lattice, Table 2, indicates that only a small percentage of iron is dissolved in ceria. This value slightly increases with the amount of Fe but still include a minority of the Fe present in the material. After aging, the increase of cell parameter indicates a segregation of the iron eventually dissolved in the lattice with formation of weak signal due to crystalline Fe_2O_3. It is known that lower valence ions such as Fe^{3+} are extremely difficult to dissolve into the ceria lattice, especially when treating at high temperature [31]. Mutual dissolution of Ce and Fe into Fe_2O_3 and CeO_2 has been reported to exist in Fe-rich Ce/Fe mixed oxides prepared by coprecipitation [32].

In order to verify the formation of solid solution we recorded and analyzed XRD features of CeO_2–ZrO_2 solid solution samples doped with rare earths and transition metals. XRD features of all fresh and calcined samples except CZF85 show only one phase, namely a cubic phases (*Fm*3*m*) of CeO_2–ZrO_2 solid solution with 48 mol% of cerium. The accuracy of the lattice constants retrieved from Rietveld refinement were estimated comparing these values with expectations from application of Vegard law assuming that all MO_x dopant (2 mol% for CZM, 5 mol% for CZF95 and 15 mol% for CZF85) were dissolved into solid solution. Table 2 compares lattice parameters retrieved from Rietveld refinement and from Vegard law. The results show a good agreement for rare earth containing materials indicating formation of ternary solid solution. The situation is different for samples containing Fe_2O_3. Values retrieved by Rietveld refinement are not in agreement with those computed from Vegard's law: the adding of a cation (Fe^{3+}) with ionic radius smaller than Ce^{4+} and Zr^{4+}, should produce a decrease in cell volume in the case of a solid solution. Conversely, we observe values higher than expected indicating that Fe_2O_3 is deposited on the surface. As in the case of pure ceria we cannot exclude that a small fraction of Fe is dissolved within ceria–zirconia framework.

3.2. Catalytic activity of ceria–zirconia based materials

Soot combustion tests were carried out either under TPO conditions in a micro flow reactor, or with a TG apparatus. Fig. 1A shows the results of soot combustion studies carried out under air in a TG apparatus over ceria and ceria–zirconia. All the catalysts examined are active in promoting soot combustion in the range of temperature from ca. 600 to 800 K. As a measure of activity we used the temperature at which 50% of weight loss is observed (T_{50}, corresponding to the temperature at which 50% of soot is converted under tight contact conditions). Similar results were also obtained by carrying out soot oxidation in a conventional flow reactor. In this case the profile of CO_2 evolved (Fig. 1B) can give us a quantitative estimation of relative activity by measuring T_m value (temperature of maximum evolution of CO_2), and although absolute values are slightly different from those obtained from TG experiments, the activity–composition curve has similar features. The values of T_m are reported in Fig. 2 against composition. For fresh CZ samples the order of reactivity is dependent on Ce content, with the lowest T_m value obtained with cerium-rich compositions. In general, when the percentage of cerium oxide decreases, in fresh samples, the temperature of oxidation increases. This result is in agreement with a previous investigations [33], where the same trend is reported. The lower activity of ZrO_2 (CZ0) is also in accordance with the study of Perrichon and co-workers [34], in which activities in soot oxidation for several supports were investigated.

After aging there is an increase of the oxidation temperature which is higher with CZ100 and CZ0; as a consequence the curve assumes an inverse volcano-type profile with a minimum in the middle composition range, characteristic of phenomena driven by the redox features of the catalyst [23]. The main difference between pure cerium and cerium–zirconium solid solution is therefore related to the stability after calcination. Pure ceria sample decreases its activity, while for solid solutions containing zirconium T_m is less influenced by calcination. CeO_2 as support in diesel soot oxidation, has been the subject of several studies [5–7,9,34,35]. Different authors agree in explaining the activity of cerium oxide with its oxygen storage capacity. One of the most important roles of CeO_2 in catalytic redox reactions is to provide surface sites [36] and to act as an oxygen storage/transport medium by its redox cycle between Ce^{4+} and Ce^{3+}. Two factors can therefore explain the behavior observed: one is the availability of surface Ce^{4+} sites and the other the ability of the material to donate its oxygen for soot oxidation. For fresh material, the amount of surface Ce sites is higher for CZ100 and CZ75 and correspondingly these samples are the most active: due to the high surface area, abstraction of oxygen involves mainly surface sites, with little or no participation of the bulk in the reaction. This can be shown in Fig. 3A where an almost linear relationship is observed by plotting the number of surface oxygen ions available for exchange [37] against T_m in fresh samples. On the contrary, after aging, the minimum T_m is found with CZ44 and CZ75 and no linear relationship is observed between surface oxygen ions and T_m. This indicates that, in

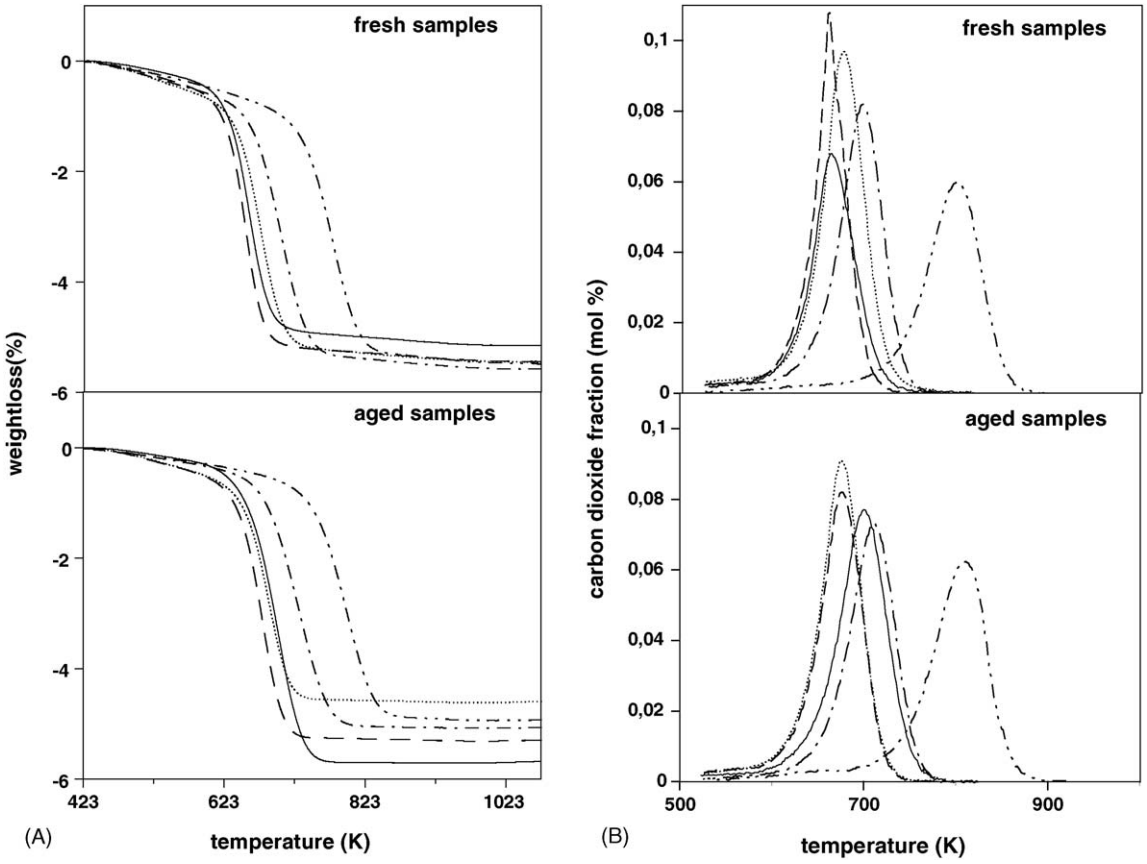

Fig. 1. Soot oxidation under stationary conditions carried out in a TG apparatus (A) and in a conventional flow reactor by monitoring evolution of CO_2 (B): (—) CZ100, (– – –) CZ75, (· · ·) CZ44, (– · –) CZ28 and (– · · –) CZ0.

addition to available surface sites, other factors should contribute to the overall oxidation behavior.

The role of oxygen storage in soot oxidation can be well evidenced by conducting a series of TG experiments in the absence of air, under inert gas flow; a sort of temperature programmed reduction under nitrogen and using soot as reductant. We used a soot/catalyst ratio of 1/115 in order to have a sufficient amount of oxygen available in the support for total oxidation of soot. The TG profiles (not reported for brevity) show a continuous weight loss starting at ca. 500 K with evolution of oxygen and CO_2. In order to exclude contributions from O_2 desorption/removal from the sample we carried out blank experiments on all catalysts by running a temperature programmed analysis in the absence of soot. The results are reported in Fig. 2B and they are compared to the behavior observed with the catalyst only treated under H_2. It is shown that for both high and low surface area samples the curve has a minimum in the middle composition range. A behavior which is similar to that observed in the presence of hydrogen, thus pointing out that participation of lattice oxygen in soot oxidation may contribute to overall activity, especially when surface area is low or in the presence of large soot particles, when access of gas phase oxygen is limited also by geometrical factors. Fig. 3B shows that there is no linear relationship in this case between the number of surface oxygen ions available for exchange and the amount of oxygen extracted as CO_2, pointing out that the lattice oxygen is directly involved in the reaction path and therefore structural features of the material play an important role.

Addition of rare earths in CZ system does not modify significantly the performance. Table 1 summarizes the TPO results of all samples, showing the temperature of maximum CO_2 evolution during soot oxidation. Activity of rare earth modified materials is close to that of ceria–zirconia and it is not influenced by calcination. This agrees with the fact that rare earth dopants are generally introduced in binary ceria–zirconia formulation to increase thermal stability. Direct promotion of OSC by rare earth doping is not straightforward and depends on several variables like preparation, textural and structural properties [38]. This could explain lack of enhanced activity in fresh samples.

Let us briefly discuss the dependence of activity against surface area. It has been recently reported that B.E.T. surface area follows a trend that is the inverse of T_{50} (or T_m) [35]; that is the surface area affects positively soot oxidation activity. This statement is true, however by plotting the difference in T_m of fresh and aged samples against surface area (Fig. 4) it is shown that for sample having surface area greater than ca. 40 m^2/g (regardless of initial surface area values) the difference in T_m (ΔT_m) is limited and generally less than ca. 20 K. On the contrary, if aging results in surface area lower than 30 m^2/g important effects in ΔT_m are observed. Therefore we can conclude that there is no linear relationship between the two

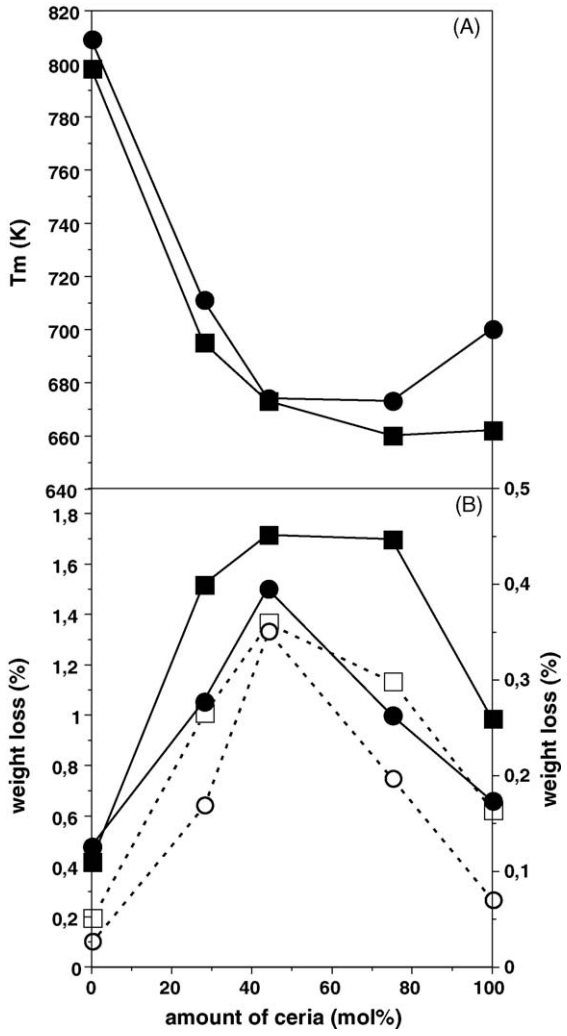

Fig. 2. (A) Correlation between T_m from TPO experiments and the amount of ceria in solid solution for both fresh (squares) and aged (circles) samples. (B) Weight loss against catalyst composition measured by TGA experiments on soot/catalyst in N_2 flow (filled symbols, left axis) and on catalyst only compositions in Ar/H_2 flow (open symbols, right axis) for both fresh (squares) and aged (circles) materials.

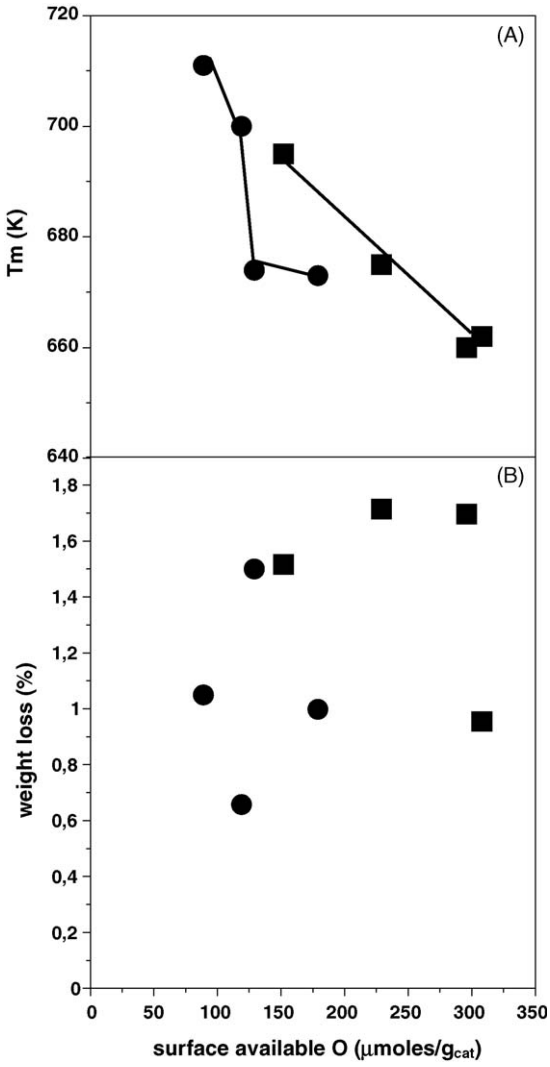

Fig. 3. Correlation between surface available oxygen and (A) T_m from TPO experiments and (B) weight loss measured by TGA experiments for both fresh (squares) and aged (circles) systems.

variables: a strong dependence is observed when ending up at low surface areas, while the activity is less influenced by even large drops in surface area, when final surface area values are higher than ca. 40 m^2/g.

3.3. The effect of doping with Fe

The results of activity of fresh and aged CF and CZF samples are reported in Table 1. The fresh sample $Ce_{0.95}Fe_{0.05}O_{1.975}$ shows the best T_m among the samples investigated (23 K lower than that of pure ceria), but a large drop of activity is observed after calcination at 1023 K. A similar situation characterizes the other Fe-doped samples. This observation led us to investigate more in detail the behavior of CF95 after aging of the sample at increasing temperature in the range 873–973 K. As shown in Table 3, the increase in calcination temperature induces a gradual loss of surface area and a corresponding increase of crystallite size. In addition it resulted in important changes in the XRD profile: the peaks of hematite and cubic ceria were narrower indicating a better crystallization of those phases (Fe_2O_3 phase was not visible in the fresh material). Moreover the unit cell parameters calculated from the reflections of cubic ceria moved from 5.4022 to 5.4100 Å, which is similar to that of the pure ceria sample. This indicates that amorphous Fe_2O_3, which was initially present on ceria, tends to crystallize and that the small fraction of Fe that was initially dissolved in the ceria lattice progressively segregates after calcination by forming free, crystalline Fe_2O_3 deposited on ceria. As shown in Fig. 5, the activity in soot combustion is strongly influenced by calcination temperature with T_m increasing by more than 100 K in the range of temperature investigated. Initially, a large drop in surface area (from 92 to 47 m^2/g) induce only a slight increase of T_m (639 K versus 646 K), on the contrary when surface area dropped below 22 m^2/g (sample calcined at 948 K) T_m raised up to 685 K. These results are consistent with our previous indications, in which it has been show that key

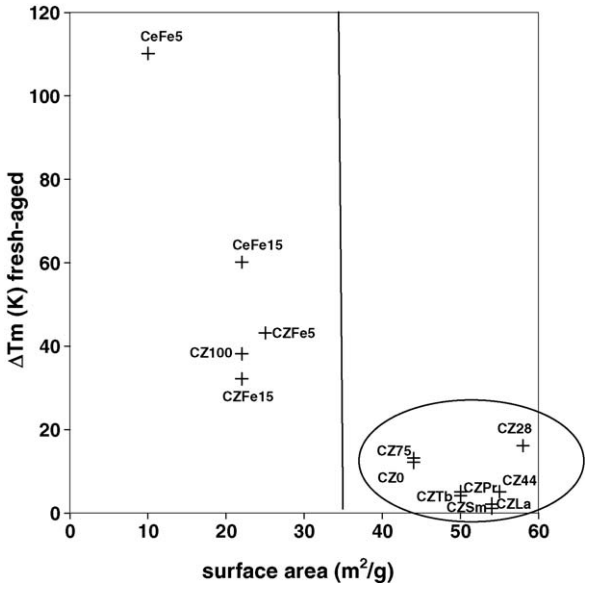

Fig. 4. Difference of T_m (ΔT_m) in aged and fresh samples from TPO experiments against surface area of the catalysts after aging. The line ideally separates the regions in which the surface area influences (left) or not (right) the activity in soot oxidation.

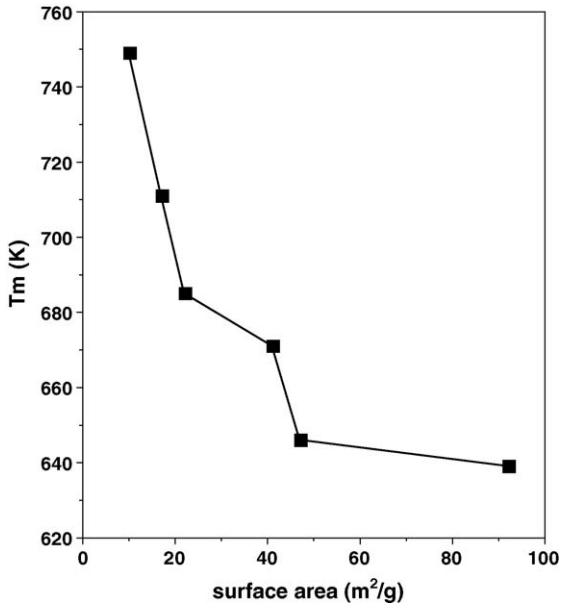

Fig. 5. Correlation between surface area and T_m returned by TPO experiments for CF95 samples calcined at different temperatures (773–1023 K).

parameter is not represented by the difference in surface area between fresh and calcined samples, but by the absolute value of surface area after calcination.

The higher activity of Fe-modified catalysts (especially CF samples) can be correlated to a high degree of Fe–Ce interaction which occurs through (i) the formation of cubic ceria-like solid solution where Fe cations are dissolved within ceria structure. In this case the interaction takes place through the sharing of oxygen anion defined by the Fe–O–Ce bonds formed in the Fe-doped CeO_2 lattice [32]. (ii) The presence of amorphous Fe_2O_3 in close contact with ceria: apart from catalytic activity deriving from CeFeO entities, the reactivity of exposed iron site within and in close contact with solid solution can have a significant role in the catalytic behavior observed. The lack of these interactions due to the lower amount of ceria can explain the different behavior of CZFe samples.

Decrease of catalytic activity after aging in samples with Fe_2O_3 has a threefold cause: segregation of Fe_2O_3 from solid solution, sintering of sample and agglomeration of free Fe_2O_3 (peaks become visible in XRD profile). These factors will weaken Ce–O–Fe interactions leading to a less active catalyst. Stabilization of these samples against sintering is therefore a key step in the development of Fe-modified cerias for application in the oxidation of soot.

Table 3
Characteristics of CF95 after aging at different temperatures

Sample	Cell parameters (Å)[a]	T_m (K)	SA (m^2/g)	Crystallite size (nm)
CF95 fresh	5.4022 (0.0004)	639	92	5.4
CF95 calc. 873 K	5.4032 (0.0002)	646	47	9.3
CF95 calc. 923 K	5.4046 (0.0001)	671	41	11.7
CF95 calc. 948 K	5.4083 (0.0001)	685	22	18.0
CF95 calc. 973 K	5.4080 (0.0001)	711	17	22.7
CF95 calc. 1023 K	5.4100 (0.0001)	749	10	44.4

[a] Obtained from Rietveld refinement.

4. Conclusion

Ceria-based materials represent an interesting class of catalysts for the combustion of soot with oxygen. Our investigation pointed out that their activity is mainly related to two factors: oxygen storage/redox capacity and surface area. An inverse dependence of T_m on surface area was observed, with the absolute value of surface area being a critical parameter: for surface area larger than ca. 40 m^2/g the variation in T_m is not relevant, while for lower surface areas a large increase of T_m is observed. The importance of lattice (surface and bulk) oxygen in ceria has been highlighted. A simple redox route mechanism for soot oxidation, which utilizes oxygen activated from the support in a typical reduction/oxidation path (Mars Van Krevelen type) in which the catalyst undergoes a partial reduction, can be put forward. Oxygen storage is therefore important because it provides an alternative route for the oxidation of big soot particles in contact with ceria.

Addition of zirconium is important to stabilize performance after calcination and to provide more reactive oxygen ions from the surface and the bulk, in a manner similar to that observed in three-way catalysts.

Fe-doped materials are the most active, but they experienced strong deactivation after calcinations. It is therefore necessary to stabilize these materials against sintering.

Acknowledgments

The authors thank financial support from MIUR (progetti PRIN). We are also grateful to Grace Davison (USA) for providing samples used in this study.

References

[1] B.A.A.L. van Setten, M. Makkee, J.A. Moulijn, Catal. Rev.-Sci. Eng. 43 (2001) 489.
[2] G. Saracco, C. Badini, N. Russo, V. Specchia, Appl. Catal. B 21 (1999) 233.
[3] P. Ciambelli, V. Palma, P. Russo, S. Vaccaro, J. Mol. Catal. A 204–205 (2003) 673.
[4] B.A.A.L. van Setten, J.M. Schouten, M. Makkee, J.A. Moulijin, Appl. Catal. B 28 (2000) 253.
[5] E.E. Miro', F. Ravelli, M.A. Ulla, L.M. Cornaglia, C.A. Querini, Catal. Today 53 (1999) 631.
[6] M.L. Pisarello, V. Milt, M.A. Peralta, C.A. Querini, E.E. Miro', Catal. Today 75 (2002) 465.
[7] V.G. Milt, C.A. Querini, E.E. Miro', M.A. Ulla, J. Catal. 220 (2003) 424.
[8] Grzona, C. Carrascull, D. Lick, M. Ponzi, E. Ponzi, React. Kinet. Catal. Lett. 75 (2002) 63.
[9] J. Setiabudi, G. Chen, M. Mul, J.A. Makkee, Moulijn, Appl. Catal. B 51 (2004) 9.
[10] Trovarelli, Comments Inorg. Chem. 20 (1999) 263.
[11] P. Ciambelli, V. Palma, P. Russo, S. Vaccaro, Catal. Today 60 (2000) 43.
[12] R. Jenkins, R. Snyder, Introduction to X-ray Powder Diffractometry, Wiley, New York, 1996, p. 90.
[13] R.A. Young, The Rietveld Method, IUCr Oxford University Press, New York, 1993.
[14] A.C. Larson, R.B. Von Dreele, General Structure Analysis System (GSAS), Los Alamos National Laboratory Report LAUR 86-748, 2000
[15] B.H. Toby, J. Appl. Cryst. 34 (2001) 210.
[16] D.J. Kim, J. Am. Ceram. Soc. 72 (1989) 1415.
[17] J.C. Summers, S.V. Houtte, D. Psaras, Appl. Catal. B 10 (1996) 139.
[18] R.J. Farrauto, R.M. Heck, Catal. Today 51 (1999) 351.
[19] M. Shelef, R.W. McCabe, Catal. Today 62 (2000) 35.
[20] G.A. Stratakis, A.M. Stamatelos, Combust. Flame 132 (2003) 157.
[21] J.P.A. Neeft, M. Makkee, J.A. Moulijn, Chem. Eng. J. 64 (1996) 292.
[22] J.P.A. Neeft, O.P. van Pruissen, M. Makkee, J.A. Moulijn, Appl. Catal. B 12 (1997) 21.
[23] E. Aneggi, M. Boaro, C. de Leitenburg, G. Dolcetti, A. Trovarelli, J. Alloys Compd. 408–412 (2006) 1096.
[24] J. Kaspar, P. Fornasiero, in: A. Trovarelli (Ed.), Catalysis by Ceria and Related Materials, Imperial College Press, London, 2002, pp. 217–241.
[25] P. Fornasiero, G. Balducci, R. Di Monte, J. Kašpar, V. Sergo, G. Gubitosa, A. Ferrero, M. Graziani, J. Catal. 164 (1996) 173.
[26] A. Trovarelli, M. Boaro, E. Rocchini, C. de Leiteburg, G. Dolcetti, J. Alloys Compd. 323 (2001) 584.
[27] V. Sanchez Escribano, E. Fernandez Lopez, M. Panizza, C. Resini, J.M. Gallardo Amores, G. Busca, Solid State Sci. 5 (2003) 1369.
[28] H. Vidal, J. Kaspar, M. Pijolat, G. Colon, S. Bernal, A. Cordon, V. Perrichon, F. Fally, Appl. Catal. B: Environ. 30 (2001) 75.
[29] E. Mamontov, R. Brezny, M. Koranne, T. Egami, J. Phys. Chem. B 107 (2003) 13007.
[30] J. Kašpar, P. Fornasiero, M. Graziani, Catal. Today 50 (1999) 285.
[31] Z. Tianshu, P. Hing, H. Huang, J. Kilner, J. Mater. Proc. Technol. 113 (2001) 463.
[32] F.J. Perez-Alonso, M. Lopez Granados, M. Ojeda, P. terreros, S. Rojas, T. Herranza, J.L.G. Fierro, M. Gracia, J.R. Gancedo, Chem. Mater. 17 (2005) 2329.
[33] J.F. Lamonier, N. Sergent, J. Matta, A. Aboukaïs, J. Therm. Anal. Calorim. 66 (2001) 645.
[34] J. van Doorn, J. Varloud, P. Meriaudeau, V. Perrichon, Appl. Catal. B 1 (1992) 117.
[35] A. Bueno-López, K. Krishna, M. Makkee, J.A. Moulijn, J. Catal. 230 (2005) 237.
[36] A. Trovarelli, Catal. Rev.-Sci. Eng. 38 (1996) 439.
[37] Y. Madier, C. Descorme, A.M. LeGovic, D. Duprez, J. Phys. Chem. B 103 (1999) 10999.
[38] R. Di Monte, J. Kaspar, J. Mater. Chem. 15 (2005) 633.